Proportional Bandwidth Properties of Fault Indicating Tones in a Ball Bearing System

M. D. Ladd & G. R. Wilson
Applied Research Laboratories, The University of Texas at Austin
Austin, TX 78713-8029

Abstract

The proportional bandwidth properties of bearing generated tones are explored in a condition based maintenance context. A comparison between time-frequency and time-scale (Wavelet) detection techniques is performed using data gathered from an experimental set up. The Wavelet techniques exhibit a 2 to 3 dB gain, depending on the harmonic number being detected.

1 Introduction

Especially in the last few years, considerable attention has been given to machinery diagnostics, i.e. methods to determine when to perform preventive maintenance on critical machinery associated with complex manufacturing or transportation systems. A recent paper from The David Taylor Research Center [1] describes the need, due to shrinking maintenance budgets, for alternative maintenance concepts and new techniques for shipboard machinery. The Navy and the Army are looking to self-monitoring capabilities for safety reasons (e.g. monitoring helicopter gear boxes [2]). Currently, preventive maintenance or preventive inspections are performed on a fixed schedule, which is determined through statistical analysis of past maintenance data. This data is based on the machinery's use, such as the number of hours of operation or the number of rotations since the last scheduled maintenance. The problem with this approach is that expensive maintenance is sometimes performed unnecessarily, or, in the worse case, failure occurs prior to the scheduled maintenance with disastrous consequences, such as a helicopter crash. A better approach is to monitor the machinery and determine when preventive maintenance is needed based on specific diagnostic criteria that accurately determine the condition of the machine. This approach, referred to as condition-based maintenance, requires detection and classification of precursors to machinery failure in time to perform maintenance. In one study, the Navy snowed a reduction of 50% for induced failures and a reduction of 35% in maintenance actions can be obtained when using condition-based maintenance [1].

Condition-based maintenance systems require a set of parameters to monitor the system and algorithms to perform diagnosis. Though several physical properties can be used as indicators (i.e., temperature, pressure, flow, oil analysis) monitoring the machine's vibrations is recognized as one of the most effective [3]. A common diagnostic method is to characterize vibrations in the frequency domain where differences between a healthy system and an unhealthy system can be detected [3] [4] . Essentially these techniques rely on detecting tones which are harmonically related to the shaft rotation rate. (However, these FFT based techniques rely on the signal's power spectrum being much larger than the noise's power spectrum at the frequencies to be detected.) Experimental results have indicated that the frequencies or tones of interest are constant Q; that is, the bandwidth of the tones increase proportionally with the harmonic number. We wish to exploit the proportional bandwidth nature of the tones for detection, which suggests the use of wavelets, since they have a constant Q resolution property [5], contrasting the fixed resolution properties of the power spectrum. The focus of this paper is to determine if the use of wavelets to exploit the constant Q nature of the tones can result in a greater probability of detection for a given signal-to-noise ratio and false alarm rate than the power spectrum.

2 Wavelet and Gabor Transform

A Wavelet Transform (WT) can be formed by taking inner products of the signal with a function, called

1058-6393/95 $4.00

the mother wavelet, scaled and time shifted:

$$X(a,b) = \frac{1}{\sqrt{a}} \left\langle x(t), h^{(a,b)}(t) \right\rangle \tag{1}$$

where

$$h^{(a,b)}(t) = h\left(\frac{t-b}{a}\right) \tag{2}$$

and

$$\langle x, f \rangle = \int x(t) f^*(t) dt. \tag{3}$$

As is well known, scaling a function in the time domain has an inverse scaling effect in the frequency domain. Therefore, when h is scaled by $0 < a < 1$, the time resolution Δt, defined by

$$\Delta t^2 = \frac{\int t^2 |h(t)|^2 dt}{\int |h(t)|^2 dt} \tag{4}$$

decreases while the frequency resolution Δf increases, which is similarly defined by

$$\Delta f^2 = \frac{\int f^2 |H(f)|^2 df}{\int |H(f)|^2 df} \tag{5}$$

where $H(f)$ is the Fourier Transform of $h(t)$

$$H(f) = \int h(t) \exp(-2i\pi ft) dt. \tag{6}$$

Their product is lower bounded by the Heisenberg inequality

$$\Delta t \Delta f \geq \frac{1}{4\pi} \tag{7}$$

and established by the mother function. Since Δf and Δt vary under the constraint of having their product set to a constant, the wavelet transform, which is a time-scale transform, has a constant Q resolution. That is, at higher frequencies, the resolution of the transform increases. The constant Q resolution property contrasts with fixed frequency resolution properties of many time-frequency transforms, such as the Gabor transform.

The Gabor Transform (GT), a windowed Fourier transform, is represented as

$$X(f,b) = \int x(t) g^*(t-b) \exp(-2i\pi ft) dt \tag{8}$$

where

$$g(t) = \pi^{-\frac{1}{4}} \exp\left(\frac{-t^2}{2}\right) \tag{9}$$

has a fixed resolution for Δf, but satisfies the Heisenberg inequality with equality. Recognizing the integral as an inner product

$$X(f,b) = \langle x(t), g(t-b) \exp(+2i\pi ft) \rangle, \tag{10}$$

ones sees that the Gabor transform can be thought of as a projection of the signal $x(t)$ onto a windowed Fourier kernel, $g(t)\exp(+2i\pi ft)$, which can be viewed as a windowing function $g(t)$ modulated by f rather than scaled by a. The resolution of the transform can be controlled by introducing a parameter α in the windowing function [7]

$$g_\alpha(t) = \sqrt{\alpha}\pi^{-\frac{1}{4}} \exp\left(\frac{-(\alpha t)^2}{2}\right). \tag{11}$$

GT_α will be used to designate this parameterized GT. As shown in [5], a mother wavelet based on Morlet's work [6] can be developed with similar frequency interpretation properties as GT_α

$$h_{(k,\alpha)}(t) = \sqrt{\alpha}\left\{ \exp(ikt) \exp\left(\frac{-(\alpha t)^2}{2}\right) - \sqrt{2} \exp\left(\frac{-k^2}{4}\right) \exp(ikt) \exp\left(-(\alpha t)^2\right) \right\} \tag{12}$$

Actually, for $k \gg 1$, the second term is numerically insignificant and at frequency $\frac{k}{2\pi}$ the two transforms will have the same frequency resolution. The WT using this mother wavelet will be designated $WT_{(k,\alpha)}$. Having the same resolution properties at a particular frequency is very important for establishing the detection properties of the WT.

3 Detection with Wavelets

In spectral based tonal detectors [8], an estimate of the power spectrum, non-stationary power spectrum, or non-stationary bispectrum is compared to a threshold to determine the presence of a signal. Theoretical distributions for the different estimates for the signal plus noise and noise only cases permit one to compute the probability of detection for a specified false alarm rate and signal-to-noise ratio. The focus here is to compare the performance of the power spectrum detector and a detector based on $WT_{k,\alpha}$. In order to apply the techniques used in [8] to the wavelet detector, the two detectors need to be put in a similar frame work.

All three of the detectors in [8] rely on the Discrete Finite Fourier Transform (DFFT):

$$X(f_l) = \sum_{j=0}^{M-1} x(t_j) \exp(\frac{-i2\pi f_l t_j}{M}), \tag{13}$$

which is used to form the desired estimate by taking the nth order cumulant. By taking a time-frequency approach and limiting the framework to the power spectrum detector, a time-frequency analysis of a signal can be created by forming periodogram estimates at discrete intervals of time. The periodogram estimates formed will then be averaged to form an asymptotically consistent estimate of the power spectrum. This approach parallels that in [8] if the time interval is such that the L estimates in time are independent. For calculation purposes, the signal $x(t_j)$ is segmented into L nonoverlapping partitions of length M:

$$x_n(t_j) = x(t_j + nb_0), \quad \begin{matrix} n = 0, 1, \ldots, L-1 \\ j = 0, 1, \ldots, M-1. \end{matrix} \tag{14}$$

The time-frequency periodogram estimate will be based on the DFFT with a windowing function $g_\alpha(t)$ defined by Eq. 11

$$\hat{X}(f_l, b_n) = \frac{1}{M} \left| \sum_{j=0}^{M-1} g_\alpha(t_j) x_n(t_j) \exp\left(\frac{-i2\pi f_l t_j}{M}\right) \right|^2, \tag{15}$$

which is a discretized form of the magnitude of $GT_\alpha(f, b)$. Likewise, a discretized form of $WT_{(k,\alpha)}(a, b)$ can be defined, but the signal partitions and thus the number of time coefficients (the number of averages) depend on the scale factor a^m. If the partitions set by Eq. 14 are used for when $m = 0$ ($a^m = 1$), and the signal length is fixed in length at $N = L * M$, then the partitioning for a particular scale factor a^m will be

$$x_n^m(t_j) = x(t_j + nb_0/a^m), \quad \begin{matrix} n = 0, 1, \ldots, \left[\frac{N}{M * a^m}\right] - 1 \\ j = 0, 1, \ldots, [M * a^m] - 1. \end{matrix}$$

Note that [ ] denotes the greatest integer function. The equivalent time-scale form of the periodogram time-frequency estimates is

$$\hat{X}(a_m, b_n) = \frac{1}{M} \left| \sum_{j=0}^{M-1} h_{(k,\alpha)}\left(\frac{t_j}{a^m}\right) x_n^m(t_j) \right|^2 \tag{16}$$

where $h_{f(k,\alpha)}(t)$ is defined by Eq. 12. The power spectrum estimate for a particular frequency f_l is formed by averaging the time-frequency plane along the time axis:

$$\hat{p}(f_l) = \frac{1}{L} \sum_{n=0}^{L-1} \hat{X}(f_l, b_n). \tag{17}$$

Similarly, an equivalent 'wavelet spectrum' estimate can be defined as

$$\hat{w}(a_m) = \frac{1}{L} \sum_{n=0}^{L_{a_m}-1} \hat{X}(a^m, b_n) \tag{18}$$

where

$$L_{a_m} = \left[\frac{N}{M * a_m}\right] \tag{19}$$

is the number of time coefficients calculated for a_m. For a given frequency f_c, $m = 0$ and $k = 2\pi f_c$,

$$\hat{w}(a_0) \cong \hat{p}(f_c) \tag{20}$$

and one can apply the same techniques for establishing the power spectrum detector's parameters and performance to the wavelet detector, that is, within reasonable numerical significance for the $\hat{w}(a_0)$ and $\hat{p}(f_c)$ bins.

A tone is detected when an estimate ($\hat{p}(f_l)$ or $\hat{w}(a_m)$) exceeds a threshold which is established for a desired false alarm rate. The threshold for $\hat{p}(f_l)$ is given by $\hat{p}^{noise}(f_l)T/2L$ where T is determined from the chi-squared distribution for the desired false alarm rate and degrees freedom $2L$ ($\hat{p}^{noise}(f_l)$ is the power spectrum estimate for the noise only case). The probability of detection for the signal plus noise is the probability that a chi-square $2L$ random variable exceeds the value $T/(r(f_l) + 1)$ where $r(f_l)$ is the ratio of the signal power to the noise power in the f_l bin

$$r(f_l) = \frac{\hat{p}^{signal}(f_l)}{\hat{p}^{noise}(f_l)}. \tag{21}$$

To set the threshold for $\hat{w}(a_m)$, one uses L_{a_m} to set the degrees of freedom and calculates $\hat{p}^{noise}(f_{l_{a_m}})$ for the partitioning defined by Eq. 14 and

$$f_{l_{a_m}} = f_c * a_m. \tag{22}$$

For the case $m = 0$ and $f_{l_{a_m}} = f_c$, the detection threshold is the same for both $\hat{p}(f_c)$ and $\hat{w}(a_0)$. For $m > 0$ (assuming $0 < a < 1$) L_{a_m} will increase, T will increase, and the noise level within the bin will increase. However, the variance of the estimate will decrease since the variance is inversely proportional to L_{a_m}, indicating the probability of detection could be improved at the higher harmonics by the wavelet detector. To confirm this conjecture, the probability of detection for both the power spectrum and wavelet detector were measured from numerical simulations using experimental data, which is described next.

4 Experimental Data and Results

Fig. 1 shows the mechanical system used for producing vibrations from a flawed bearing. The inner

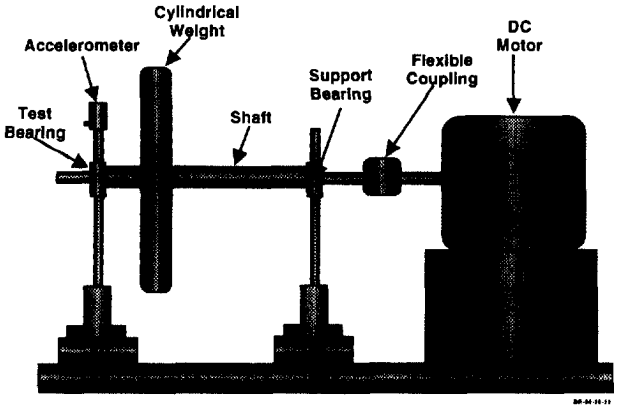

Figure 1: Test Apparatus.

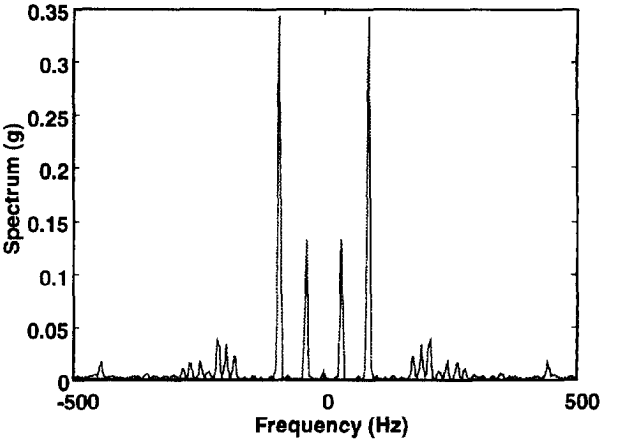

Figure 2: Data Spectrum.

SNR	Power Spec.		Wavelet	
	Pd	Conf.	Pd	Conf.
-3.1	0.03	0.01-0.08	0.03	0.01-0.08
-0.2	0.23	0.16-0.32	0.23	0.16-0.32
2.7	0.86	0.78-0.91	0.86	0.78-0.91
6.1	1.00	0.96-1.00	1.00	0.96-1.00

Table 1: Fundamental Harmonic Detection Results

and outer race of the bearing were etched with a Dremel tool using a dental burr in order to simulate spalling and inner/outer race out of roundness effects. To provide a fairly stable rotation rate, a D.C. motor with a shaft rotation rate of 35 Hz was used to drive the flawed bearing. As indicated, a rubber, flexible coupling connected the D.C. motor to the drive shaft in order to reduce the injection of motor vibrations into the measuring system. The accelerometer was mounted in the vertical axis to the test bearing support. The mounting screw was in contact with the bearing's outer casing as well as the accelerometer.

The analog accelerometer data was filtered with a 12 dB roll off after the passband of 0 to 1100 Hz. Digitizing was done by a NB-A2000 Lab View card mounted in a Quadra 700 with a sampling rate of 3600 Hz.

Fig. 2 shows the power spectrum of the data and Fig. 3 shows the power spectrum of the fundamental and eighth harmonic of the shaft rotation rate in greater detail ($M = 2^{17}$). One can see that the eighth harmonic's bandwidth does span more than one DFFT bin while the fundamental is almost contained in a single bin. The $*$ indicates a point within three dB of the tone's peak.

Simulations using these tones with normal (unit variance, Gaussian) white noise added were performed: one set measuring the probability of detection for $f_c = 35$ and $a_0 = 1$ at various SNRs, and the second for the eighth harmonic $f_{l_h} = 8 * f_c$ and $a_{m_h} = \frac{1}{8}$. The DFFT length was set at $M = 2^{17}$ which set the resolution of the DFFT to almost match that of the tone at 35 Hz (Fig. 3). The signal to noise ratio as defined by Eq. 21 is established by scaling the data series by an appropriate factor to produce the desired value for $r(f_0)$ or $r(f_{l_h})$. This scaling proceedure doesn't produce the desired SNR exactly, thus the SNR given in the results is calculated from

$$SNR(f_l) = 10 \log \left(\frac{\hat{p}^{signal+noise}(f_l)}{\hat{p}^{noise}(f_l)} - 1 \right). \quad (23)$$

Setting the SNR by scaling the data rather than adjusting the noise variance allows one fix the detection threshold for all the tests. The threshold is set theoretically from the noise only probability density function for a false alarm rate of 10^{-3}.

Table 1 shows the measured probability of detection for $f_c = 35$ and $a_0 = 1$ at various SNRs (Eq. 23) with the 95% confidence intervals. One hundred trials were used to estimate the probability of detection. The results are identical since the resolution of the two transforms are the same at this frequency. Table 2 shows similar results for $f_{l_h} = 8 * f_c$ and $a_{m_h} = \frac{1}{8}$. The probability of detection for the wavelet detector is greater than the probability of detection for the power spectrum detector. The wavelet detector obtains a near one probability of detection at an SNR of 3 dB while the power spectrum detector takes an SNR of 6

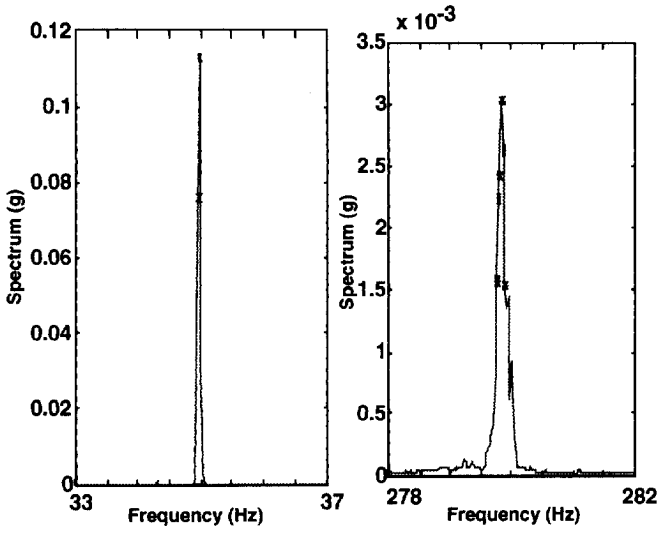

Figure 3: Power Spectrum of the Fundamental and 8th Harmonic.

SNR	Power Spec.		Wavelet	
	Pd	Conf.	Pd	Conf.
-3.1	0.05	0.02-0.11	0.15	0.09-0.23
-0.1	0.31	0.23-0.41	0.49	0.39-0.59
3.0	0.82	0.73-0.88	0.99	0.95-1.00
6.1	1.00	0.96-1.00	1.00	0.96-1.00

Table 2: 8th Harmonic Detection Results

dB to obtain a probability of detection of one. Though the table does not include detection estimates for 4 and 5 dB, theoretically, one would expect the power spectrum to approach one between 5 and 6 dB [8]. One can estimate an improved detection performance of 2 to 3 dB (in SNR) for the wavelet detector.

5 Summary and Conclusions

In this paper, we have presented the concept of a wavelet detector for detecting constant Q narrowband tones. A framework based on time-scale and time-frequency concepts was developed in order to draw comparisons to the power spectrum detector. Actual data, derived from vibrations created by a flawed ball bearing in an experimental system was used to compare the two detectors. Since the wavelet detector reduces the variance of the signal plus noise for the higher harmonics when compared to the power spectrum detector, it was shown that better detection performance of 2-3 dB can occur. The performance could be enhanced even further if overlapped partitions of the data were used, which is what we are currently looking at.

Acknowledgments

This work was supported by the Independent Research Program at Applied Research Laboratories, The University of Texas at Austin, Austin, Texas and the Office of Naval Research.

References

[1] Nickerson, G. W. and C. P. Nemarich (1990). "A Mechanical System Condition-Based Maintenance Demonstration Model," *IEEE System Readiness Technical Conference AUTOTESTCON '90*, 529-33.

[2] Rock, D., D. Malkoff, and R. Steward (1993). "I and Aircraft Health Monitoring," *AI Expert 8(2)*, 28-35.

[3] Wowk, V. (1991). *Machinery Vibration, Measurement and Analysis.* McGraw-Hill, Inc., New York, N. Y.

[4] Berry, J. (1991). "How to Track Rolling Element Bearing Health with Vibration Signature Analysis," *Sound and Vibration*, Nov, 24-35.

[5] Ladd, M. and G. Wilson (1993). "Frequency Resolution Properties of the Wavelet Transform for Detecting Harmonically Related Narrowband Signals," *Proceedings of the 1993 International Conference on Acoustics, Speech, and Signal Processing*, Minneapolis, MN.

[6] Goupillaud, P., A. Grossmann, and J. Morlet (1984/85). "Cycle-Octave and Related Transforms in Seismic Signal Analysis," *Geoexploration*, Vol. 23, 85-102.

[7] Harris, Fredric J. (1978). "On The Use of Windows for Harmonic Analysis with the Discrete Fourier Transform," *Proceedings of the IEEE*, Jan, 51-83.

[8] Wilson G., Hardwicke K. R. and R. T. Trochta (1993). "Coherent Harmonic Detection Using Non-Stationary Higher Order Spectra," *Proceedings of the 1993 International Conference on Acoustics, Speech, and Signal Processing*, Minneapolis, MN.